Kinetics and Thermal Crystallinity of Recycled PET. II. Topographic Study on Thermal Crystallinity of the Injection-Molded Recycled PET

DAW-MING FANN, STEVE K. HUANG, and JIUNN-YIH LEE*

Graduate School of Textile and Polymer Engineering, National Taiwan Institute of Technology, Taiwan, Republic of China

SYNOPSIS

The injected specimens of recycled poly(ethylene terephthalate) (R-PET) and its blends with engineering PET (E-PET) are studied with differential scanning calorimetry (DSC). Specimens are dissected into three segments of (1) outer skin, (2) middle, and (3) the core for the topographic study of their separate crystallinities, which are induced by different crystallization rates in the injection mode. DSC thermograms reveal the different crystallinity states among these three segments with decreasing crystallinity from core to middle to the skin segments and the times and contact of injection-molded specimens with the mold during the cooling cycle after the injection of the specimens. With the same procedures of injection molding, comparisons of crystallinity among various specimens of virgin blow molding grade PET (B-PET), E-PET, and R-PET are made. There are little differences in crystallinity among three segments of B- or E-PET specimens. In contrast, a higher degree of crystallinity in the core segment than either middle or skin segments is observed for the R-PET. This may contribute to the faster crystallization rate of the R-PET in the mold. Specimens of R-/E-PET blends follow the R-PET pattern, even in 20% of R-PET in the blend. This faster crystallization rate of R-PET is confirmed with the lowering crystallization temperatures (T_c) of the R-PET and R-/E-PET blended specimens in the DSC heating process. Dynamic DSC cooling analysis reveals a high order of crystallinity in R-PET and R-/E-PET blends. Gel permeation chromatography (GPC) measurements of molecular weights and distributions support the orderly structure for R-PET. Terminal group analysis and intrinsic viscosity measurements of the R-PET support the chain modification of R-PET during the thermal treatments in accordance with the evidences of smaller M_w and narrower molecular weight distribution from the GPC findings for the recycled PET. © 1996 John Wiley & Sons, Inc.

INTRODUCTION

The recovered poly(ethylene terephthalate) (R-PET) material from beverage bottles has found many applications, from the use of engineering PET (E-PET) to outdoor well-worn hiking boots, rugged sweaters, and most garments made of polyester. The blending of virgin PET and recycled PET (R-PET) has been the worldwide trend in many applications.[2] The dynamic crystallization kinetics of R-PET and R-/E-PET blends were reported and discussed in part I of this series.[1] In this study, the objective is to examine the crystallization behavior of recycled PET and its blends with engineering PET in injection molding applications.

The crystalline structure and morphologies formed in injection moldings of semicrystalline polymers have been reviewed by Katti and Schultz.[3] Other studies have been concerned specifically with injection-molded polypropylene (PP),[4,5] high-density polyethylene (HDPE),[6] and pigmented polyolefins.[7] Morphological evidence of the injection-

* To whom correspondence should be addressed.

Journal of Applied Polymer Science, Vol. 61, 261–271 (1996)
 CCC 0021-8995/96/020261-11

molded polymer often displaces zones that Katti and Schultz described as (1) skin, (2) middle, and (3) core. Material in the outer layer which contacts the mold wall is labeled as skin zone, and deep center as the core and middle zones in between. Each receives variable shear flows in the making and temperature gradients during the cooling of the mold. Skin zone is subjected to high shear and rapid chill of the mold, and the effects are gradually diminished from the middle to the core. The crystalline structure may form in row-nucleated fashion due to a lack of time for the skin and slower cooling condition, which allows time for more orderly crystalline structure for the core.[3]

It is our interest to evaluate the crystallization behaviors of R-PET and its blends in three zones, as described, and to find the cause or to obtain further evidence for the high crystallinity of R-PET and its blends which stem from the thermal treatment in the recovery process of the PET material. In doing so, molecular weight and distribution measurements by GPC and end-group analysis of R-PET are performed and results are discussed.

EXPERIMENTAL

Materials

The PET sample bars were made by the injection-molded process. The materials used for this study and the injection conditions were discussed in part I[1] of this study and are described here in Table I.

Differential Scanning Calorimetry

A Perkin-Elmer DSC-7 instrument was used. The samples were weighted in the aluminum sample holder. The calorimeter was operated with a stream of oxygen-free dry nitrogen flowing over the sample and the reference. All samples were previously kept in a room-temperature vacuum oven before test. The DSC runs were made at heating rate of 10°C/min within a temperature range of 40 to 294°C. The recorded thermograms were used for calculations of all the first-order and second-order transitions, including glass transitions, crystallization, and fusion. The definitions of terms used are according to ASTM D3418. Calculation of the degree of crystallinity K was as follows:

$$K = (\Delta H_{melt} - \Delta H_{cryst})/\Delta H_{literature(145\ J/g)} \times 100\%$$

To reveal the degree of crystallinity at different sites in an injected mold, a topographic sampling technique was used by a razor blade, as shown in Figure 1.

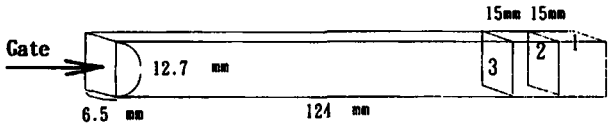

Figure 1 Schematic illustration of the sections taken from the injection-molded bars. (1) Skin, (2) middle, (3) core.

Viscometry

PET (0.5 g) was dissolved in 50 mL of 60 : 40 W/W phenol : tetrachloroethane at 80°C for 30 min, and the viscosity was measured using an Ubbelohds viscometer. Flow times were obtained at 25°C; values of the intrinsic viscosities (IV) were obtained from standard calibration graphs.

Gel Permeation Chromatograph

The molecular weight determinations were acquired with a Waters 150-C gel permeation chromatograph with a refractive index detector and data module. Samples were dissolved and filtered in 98 : 2 w/w Hexafluoroisopropanol (HFIP) : chloroform, with a concentration of 2 mg/mL. An injection volume of 0.1 mL and elution volume of mobile phase of 1 mL/min were used.

End-Group Determination

End-group determination followed the method described by Conix.[8] The polymer sample (1 g finely

Table I Composition of PET Injected Bars

B-PET	R-PET	E-PET	R20/E80	R50/E50	R80/E20
Blowing Grade PET	Recycled PET	Engineering Grade PET	Engineering/recycled PET blends		

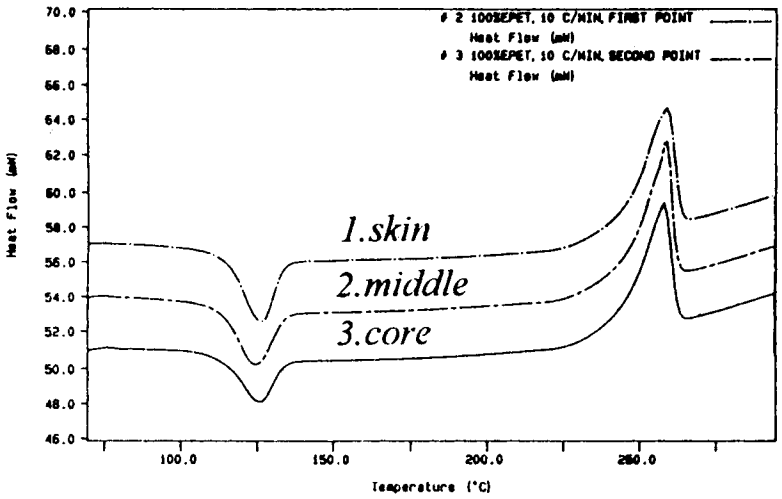

Figure 2 DSC curves of E-PET from various positions of injected mold.

ground chips) was refluxed in 15 mL *o*-cresol : chloroform 7 : 3 (by weight) mixture under an N_2 atmosphere for 2 h at 85°C. The solution obtained was cooled at 40°C, and 5 mL of *o*-cresol : chloroform 7 : 3 mixture was added. Titration was carried out with a 0.1*M* solution of potassium hydroxide in benzyl alcohol using 0.1% of phenol red in ethanol as indicator.

Color Measurement

A Minolta CR 300 color measuring system was used to measure the color of injected samples. Definitions of terms are in according to CIELAB color coordinates. A C illuminant and 2-degree viewing angle were used in all measurements and calibrated using a Minolta white reference standard 2″ diameter. The 3-mm-thick injection-molded round samples were measured with a white background.

RESULTS AND DISCUSSION

Topographic Study of the Blended R- and E-PETs

The crystallization behaviors of the recycled PET (R-PET) and R-/E-PET blends are found with faster crystallization rates and higher-order crystalline structures than the virgin PET, as discussed in Part I.[1] This behavior of crystallization upon the cooling mode study of the DSC may be understood further if the injection-molded sample

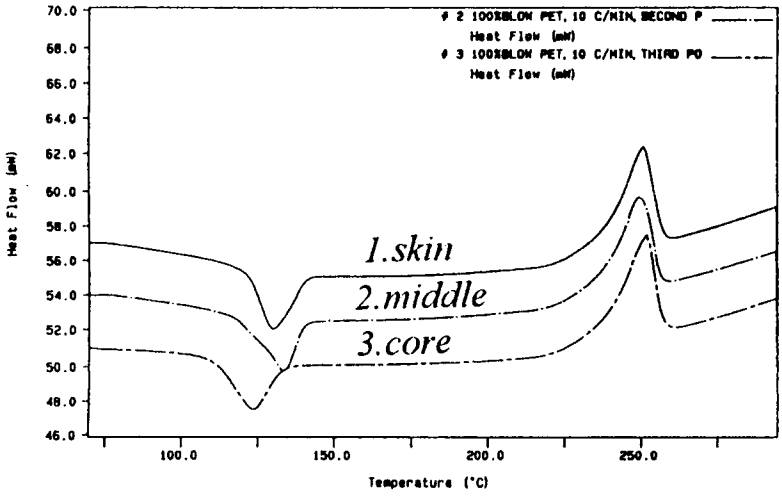

Figure 3 DSC curves of B-PET from various positions of injected mold.

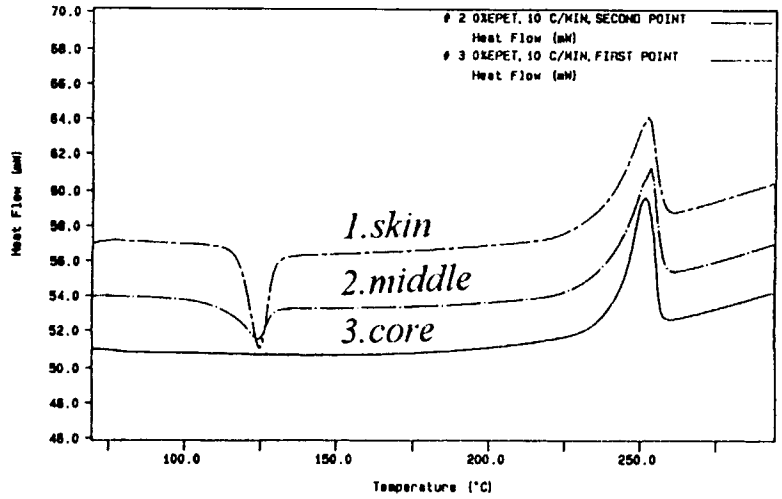

Figure 4 DSC curves of R-PET from various positions of injected mold.

is dissected into thinner segments and the crystallization behaviors which are dictated by temperature gradient and melt flow are observed with these thin segments. The sample of the three segments of (1) skin, (2) middle, and (3) the core is shown in Figure 1.

The heat profiles of ΔH_c (enthalpy dissipation of crystallization) with the three segments of skin, middle, and core of an engineering PET (E-PET) are shown in Figure 2. The similarity of the three curves of (1) skin on the top and (2) middle and (3) core on the descending order shows that the heat dissipation (ΔH_c) on these three segments are rather similar but with slight decreases in the T_c ranges from the skin to middle to core. This obvious heat dissipation of the E-PET material indicated that the molecular chains in sample form of the injection molding were rather strained in various degrees depending on the locations and upon reheating on the DSC run. The energy was then released as the crystalline structure was formed at the T_c temperature range. Since the skin of the specimens was cooled faster than the middle or the core, a larger segment of the skin of the specimens was in amorphous fashion than the middle and the core. With this consequence and reflection, the ΔH_c was found to be the largest in the skin and gradually decreased in the middle and the core accordingly. With the slower heat dissipation in the body of the segment of the specimen, the crystallization of the middle and the core segments may proceed with more available time before the cooling takes place.

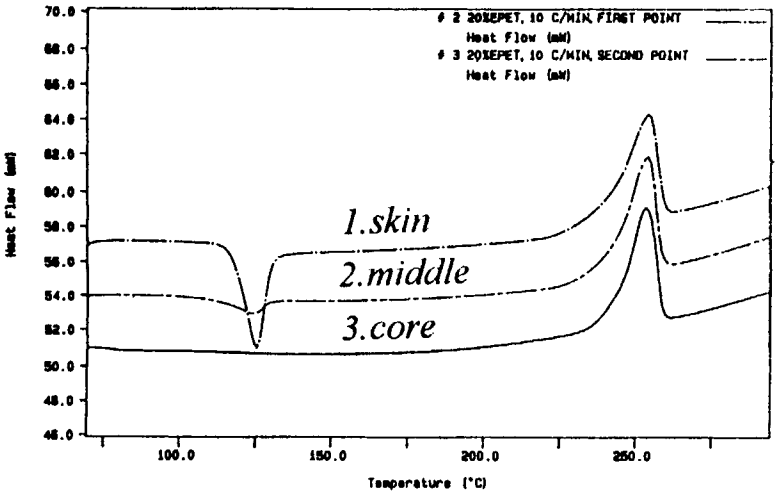

Figure 5 DSC curves of R80/E20 PET from various positions of injected mold.

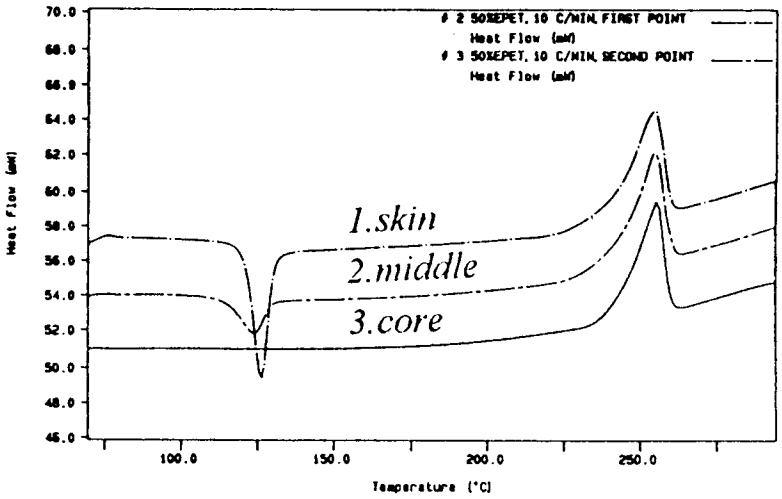

Figure 6 DSC curves of R50/E50 PET from various positions of injected mold.

With this general relationship of heat of dissipation versus the crystallization process in order, further examinations of other injected PET samples were taken. They are shown in Figure 3 for the 100% virgin blow-molded PET (B-PET), Figure 4 for 100% recycled PET (R-PET), and Figures 5, 6, and 7 for the 80%, 50%, and 20% of the recycled PET in the blends of R-/E-PET samples, respectively.

In Figure 3, the PET bottle species (B-PET, PET bar injected with virgin blow-molding materials) showed the thermal behavior of broader T_c and more heat dissipation. The molecular chains were rather strained and amorphous in nature, coincident with their transparent appearance. Molecular chains strained from skin to core reflect the lower crystallization rate.[1]

On the other hand, the better heat annealing processes for the recycled and blended PET materials are observed in Figures 4 through 7. Flat or nearly flat T_c ranges of the core (bottom curves) of the samples are observed.

The skin and middle segments of the recycled PET material in 100% form or in blends, as shown in Figures 4 through 7, showed a distinct difference in the T_c ranges with a larger ΔH_c for the skin segment and much smaller ΔH_c for the middle segment.

The contrast behaviors of the core and even the middle segments in different samples of E- and B-PET to the R-PET and R-/E-PET blends indicate the ease of the crystallization of the recycled material, even in the blended forms with the E-PET material.

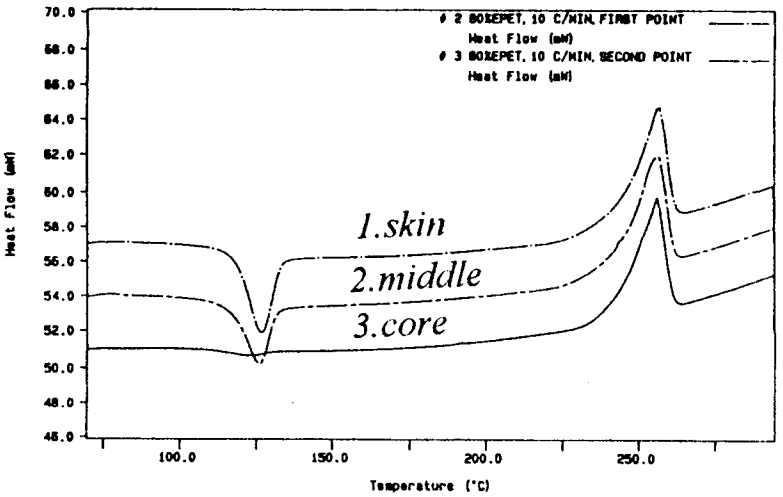

Figure 7 DSC curves of R20/E80 PET from various positions of injected mold.

Table II The Crystallinity of the Different Segment of Injection-Molded Samples

Sample	Position[a]	ΔH_c (J/g)	ΔH_m (J/g)	Cryst. (J/g)	K (%)
B-PET	1	−27.23	42.54	15.32	10.56
	2	−26.23	42.15	15.92	10.98
	3	−23.80	43.48	19.68	13.57
E-PET	1	−28.89	50.24	21.36	14.73
	2	−26.83	50.28	23.45	16.17
	3	−21.06	48.63	27.57	19.02
R20/E80	1	−28.75	45.86	17.11	11.80
	2	−22.53	45.44	22.91	15.80
	3	−3.12	41.53	38.41	26.49
R50/E50	1	−30.28	45.76	15.48	10.68
	2	−13.14	44.45	31.31	21.59
	3	—[b]	39.29	39.29	27.10
R80/E20	1	−30.04	46.67	16.63	11.47
	2	−6.43	44.82	38.39	26.21
	3	—[b]	43.19	43.19	29.78
R-PET	1	−27.67	42.77	15.10	10.41
	2	−13.33	42.76	29.43	20.29
	3	—[b]	43.63	43.63	30.09

[a] Segment position illustrated in Figure 1.
[b] Negligible.

The skin segment of the recycled PET was greatly affected by the cooling process of the injection-molding procedures on making of the samples. With the contact of the cold surface of the mold, the R-PET was unable to form the crystalline form with the mold contact and the mold efficiency upon removal of the heat. Therefore, upon reheating in the DSC runs, a great deal of energy was released as the strained or amorphous moieties were quickly changed to the crystalline forms. The sharpness and the narrow T_c temperature ranges indicate the faster crystallization rates of the R- and R-/E-blended samples.[1] The degrees of crystallinity of the segments of (1) skin, (2) middle, and (3) core are shown in Table II.

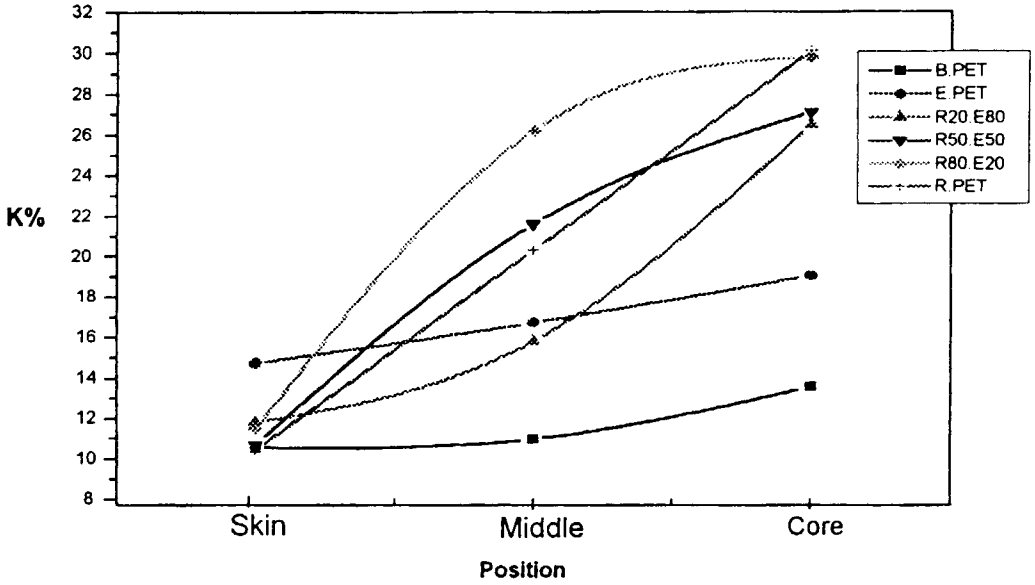

Figure 8 Degree of crystallinity distribution at different positions in injected mold of recovered and blended PET.

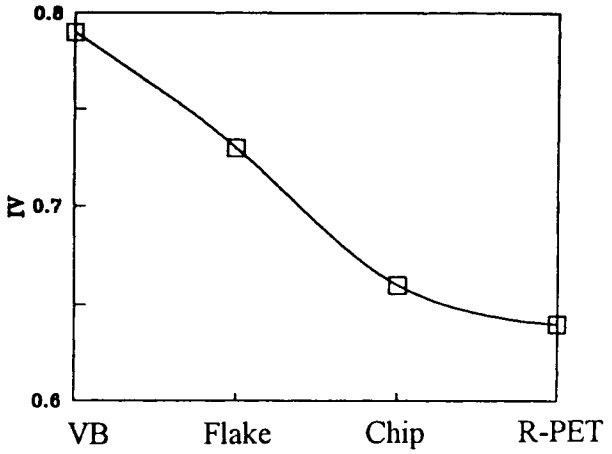

Figure 9 IV change of blow-molding PET after recovered process.

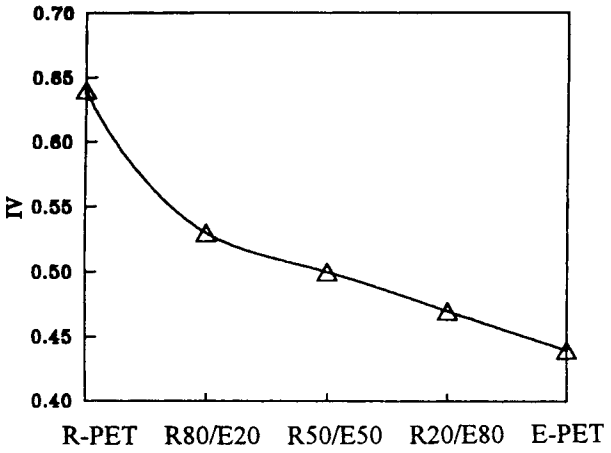

Figure 10 IV measurement of R-/E-PET blends.

From Table II and Figure 8, the core has ΔH_c of 3.12, and the middle segment has 22.53 and skin has 28.75 J/g for the R20/E80 sample. This general trend is observed in other samples as well. With more time available at the lower heat dissipation segment, higher crystallinities are observed. K values in % for core, middle, and skin segments of the R20/E80 are 26.49, 15.80, and 11.80, respectively.

From Figure 8, the sharp increase of the crystallinity, as measured in T_c range, indicates that the recycled PET material (the 80% R-PET in the blend and the other blends) may act as a crystallization promoter to ease the strains of the blending upon reheatings of the blended samples. The high degree of crystallinity that occurred at the core segment reflects the faster crystallization rate for these blends. These results are in accordance with the findings from the previously described dynamic crystallization kinetics on the samples.[1]

Molecular Weight Measurements of the R-PETs

Intrinsic viscosities (IVs) of the samples of the virgin blow-molding resin (VB), crashed bottle flakes (flake), extruded chip (chip), and injected samples of E-PET as well as R-PET and its blends of 80%, 50%, and 20% of R-PET in R-/E-PETs were measured, and the results are shown in Figures 9 and 10 and listed in Table III.

A few observations are in order. First, the intrinsic viscosities of the PET of the original blow-molded resin (VB), bottled and crashed (flake), and extruded (chip) were decreased as the thermal process cycles were increased, as shown in Figure 9. Second, the IVs were in accordance with the proportional contents of the two components in the blended samples, as shown in Figure 10. Third, the smooth and expected measurements of the IVs of the materials indicate the change of crystallization behaviors which are not due to the severe incision of the molecular chains upon the thermal process. There may

Table III Molecular Weights and Distributions of the PETs

	VB	Flake	Chip	R-PET	R80/E20	R50/E50	R20/E80	E-PET
M_n (10^4) measured	2.27	2.15	1.86	1.70	1.60	1.43	1.38	1.36
M_n (10^4)[a] calculated	2.19	1.98	1.79	1.90	1.42	1.23	1.18	1.11
M_n (10^4)[b] calculated	2.35	2.13	1.87	1.80	1.42	1.32	1.23	1.13
M_w (10^4) measured	4.82	4.49	3.65	3.20	2.84	2.68	2.45	2.31
M_w (10^4)[a] calculated	4.67	4.13	3.53	3.37	2.52	2.31	2.10	1.89
M_w (10^4)[b] calculated	4.99	4.44	3.69	3.19	2.51	2.47	2.17	1.93
Dispersity measured	2.13	2.09	1.97	1.77	1.77	1.87	1.77	1.71
$[\eta]$ measured	0.79	0.73	0.66	0.64	0.53	0.50	0.47	0.44

[a] Calculated with eq. (1)[10] and measured dispersity.
[b] Calculated with eq. (2)[11] and measured dispersity.

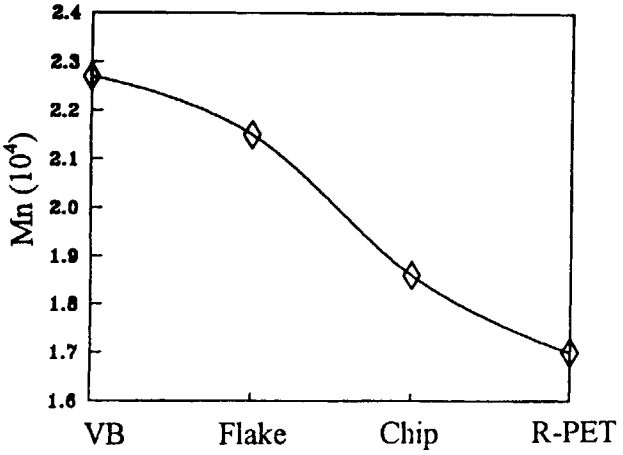

Figure 11 M_n change of blow-molding PET after recovered process.

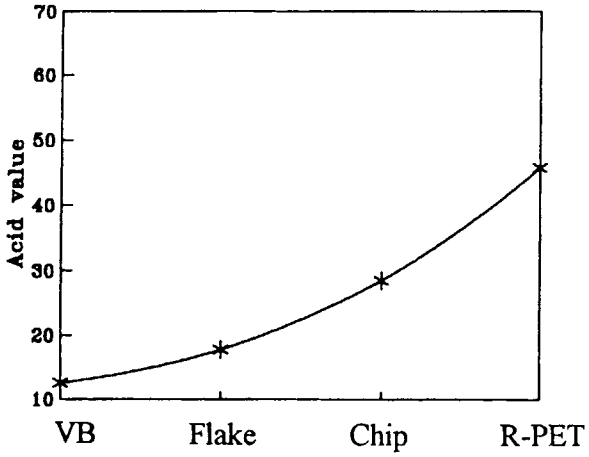

Figure 13 Acid value change of blow-molding PET after recovered process.

be a thermal amending process, in which the molecule threads protruding from entanglements are attacked and break off during the thermal recycling process.[9] To verify this, GPC measurements were carried out for the measurements of the molecular weights of these PETs and are listed in Table III.

The engineering PET used in this study has a lower molecular weight than the recycled PET. The same low molecular weights of E-PET are obtained in its intrinsic viscosity measurements. The high specifications of the blow-molding grade of PET which is required for the making of PET beverage bottles is observed with high M_w and M_n and broad molecular distribution. The molecular weight of the VB is the highest. The M_w values ($\times 10^4$) of 4.82 of the VB, the virgin material, were 4.49, 3.65, and 3.20 for the flake, chip and R-PET, respectively, and the decreasing values of M_n ($\times 10^4$) were also found to be 2.27 (VB), 2.15 (flake), 1.86 (chip), and 1.70 for the R-PET, respectively. These molecular weight decreases were shown in Figures 11 and 12.

The M_w/M_n ratios for these samples were also in descending values from 2.13 for VB, to 2.09 for flake, to 1.97 for chip, and reached the rather steady value of 1.77 for the recycled and blended PET.

These results confirm that the molecular weights are decreased through the thermal process, as indicated in the previous intrinsic viscosities measurements, and the molecular distribution gets narrower, as indicated by the M_w/M_n values.

The relationship between viscosity of PET polymer solution and GPC molecular weight measurement with the Mark-Houwink equation was examined. The Berkowitz equation[10] relates the intrinsic viscosity [η] of PET to its M_w:

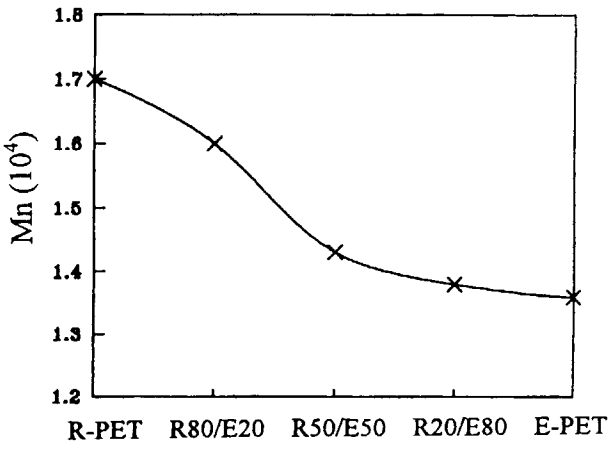

Figure 12 M_n measurement of R-/E-PET blends.

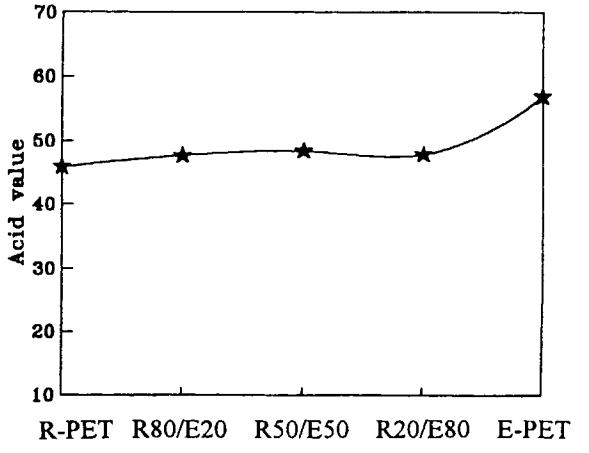

Figure 14 Acid value measurement of R-/E-PET blends.

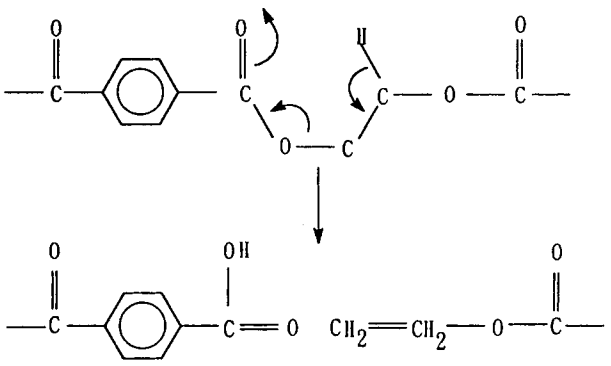

Figure 15 Formation of the carboxylic end group via thermal degradation.

$$[\eta] = 7.44 \times 10^{-4} M_w^{0.648} \quad (1)$$

The Uglea equation[11] relates the intrinsic viscosity to M_n:

$$[\eta] = 2.52 \times 10^{-4} M_n^{0.80} \quad (2)$$

The measured data and calculated molecule weights and distributions from the preceding equation are listed in Table III.

For instance, the M_n ($\times 10^4$) of R-PET is 1.70 (GPC measured), 1.90 [calculated from the measured [η], dispersity, and eq. (1)], and 1.80 [calculated from the measured [η] and eq. (2)]. The M_w ($\times 10^4$) of R-PET is 3.20 (GPC measured), 3.37 [calculated from the measured [η] and eq. (1)], and 3.19 [calculated from the measured [η], dispersity, and eq. (2)]. As a result, the Uglea equation of measurement of [η] based on the M_n is more closed related than the M_w of the Berkowitz equation.

To further verify the molecular redistributions, end-group analysis was then carried out.

Table IV CIE Color Absolute Data for Injection-Molding Sample

	L^*	a^*	b^*
B-PET	76.35	0.70	0.68

End-Group Determinations

The PET structure is represented in Figure 15. The end groups of either hydroxyl from the glycol or carboxylic acid group from phthalic moieties may be presented in the oligomers of the PETs. The mechanisms of thermal degradations of PET and PBT have been studied for many years with the help of well-chosen model compounds.[12-14] Buxbaum[12] and Zimmermann[13] stated that the primary step is an ionic process, a β—CH hydrogen transfer leading to

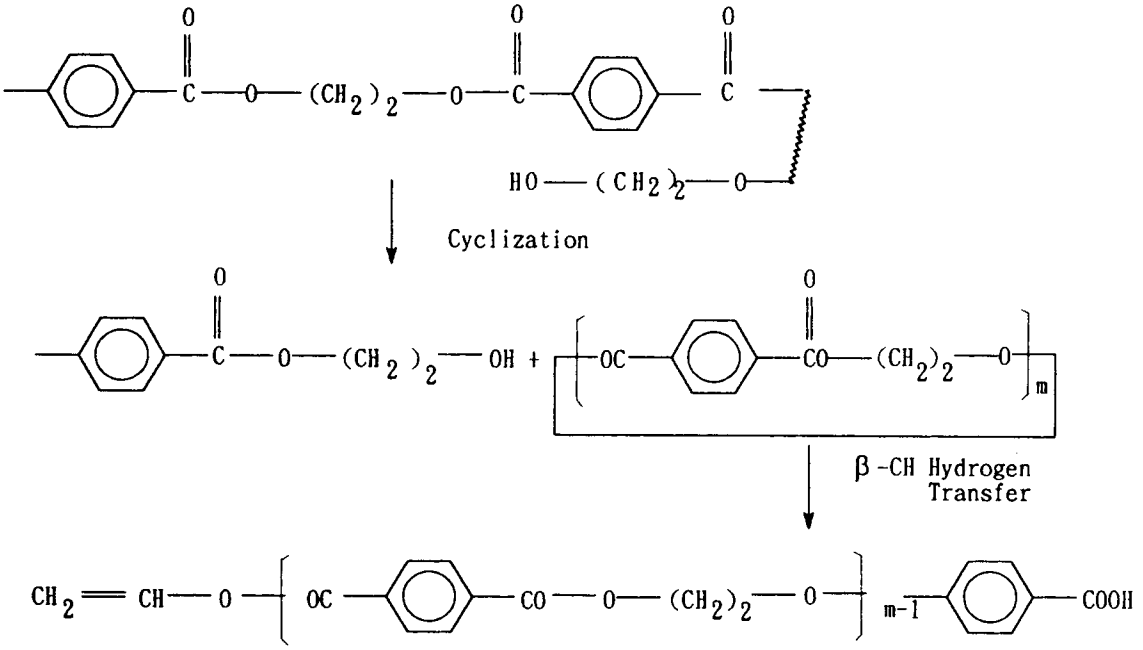

Figure 16 Cyclicization of the thermal degradation mechanism of PET.

Table V CIE Color Difference Data for Various Injection-Molding Samples

	ΔL^*	Δa^*	Δb^*	ΔE^*
B-PET	0.00	0.00	0.00	0.00
R-PET	−23.63	0.63	12.43	26.71
R80/E20	−15.15	−2.05	6.69	16.69
R50/E50	−14.97	−2.51	4.15	15.74
R20/E80	−17.28	−0.42	7.39	18.80
E-PET	−10.05	−0.73	6.40	11.93

the formation of oligomers with olefin and carboxylic end groups (Fig. 15).

Further studies[15–17] have established that the cyclization occurs in PET through an intramolecular alcoholysis reaction (ionic), which is activated in the temperature range of 250–300°C, implying the attack of hydroxyl ends on the inner ester groups of the polyester chain (Fig. 16).

The carboxylic acid group was determined by alkali titration, and the results are shown in Figures 13 and 14. The acid values (eqw/10^6) were increased from 12.6 for the VB, to the 17.8 for flake, and 28.5 for the chip materials. For the more thermally processed materials, the higher the acid values are indicated.

The recycled PET shows great increases in acid value (eqw/10^6) from 12.6 of the virgin bottle material (VB) to 45.8 for the R-PET. and 47.7, 48.4, 47.9, and 56.9, respectively, for 80%, 50%, 20%, and 0% (E-PET) of the R-PET in the R-/E-PET blends. The engineering PET material used has an acid value of 56.9. Figures 13 and 14 show the increasing acid values of the recycled and blended samples.

The chemical analysis of the recycled PETs indicates that minimum damages occurred during the recycling process and that the recovered materials are somewhat modified for these PET materials. The increase of the acid value is two- to fivefold and is within the application ranges for the engineering plastics of the PET.

Based on these molecular weight and distribution measurements by GPC and the chemical conformations of the increasing end groups, better mechanical properties may be derived from chain-length modification of too-long segments to give better chain lengths for engineering applications with the narrower yet excellent molecular distribution in the thermal processes of the recycled PET materials.

Color Measurement

The unsaturated and carboxylated termination units formed by the degradation of ester groups may be important in the colorization of the PET. CIELAB color coordinate measurement is used to characterize the color changing of recycled and blended process. The L^* value represents the lightness of sample. A perfect white has an L^* value of 100, while a perfect black has a value of zero. The quantities a^* and b^*, called opponent coordinates, define the degree of yellowness (positive b^*), blueness (negative b^*), redness (positive a^*), and greenness (negative a^*). Colorimetric data are listed in Tables IV and V.

As shown in Table V, color changes of recovered process (R-PET) and R-/E-PET blends are detectable. These colorimeter data suggest that R-PET appear yellower (higher b^* value) and duller (lower L^* value), and all blends are getting more or less in yellow tone and less bright. The colorimetric data were also consistent with visual examination.

CONCLUSION

Topographic studies of the recycled PET materials in skin, middle, and core segments confirm the faster crystallization rate and better crystalline structure for recycled PET materials. The GPC and end-group measurements of recycled PET indicate that chain modification may take place only for very long or cumbersome segments of the chains. Good-sized chains were produced as the narrower molecular distribution was found. The DSC crystallization study indicates that recycled PET material is as good as any engineering grade, if not better, for some applications, such as the ease of crystallization and processing.

The authors are grateful to Shin-Kong Synthetic Fibers Corp., Taiwan, for their generous help with the measurements of GPC, intrinsic viscosity, and end-group determination. The PET raw materials used in this study were also provided by Shin-Kong Corp.

REFERENCES

1. D. M. Fann, S. K. Huang, and J. Y. Lee, *J. Appl. Polym. Sci.*, to appear.
2. R. D. Leaversuch, *Modern Plast. Int.*, **July**, 40 (1994).
3. S. S. Katti and J. M. Schultz, *Polym. Eng. Sci.*, **22**, 1001 (1982).

4. M. W. Murphy, K. Thomas, and M. J. Bevis, *Plast. Rubb. Proc. Appl.*, **9,** 3 (1988).
5. M. R. Kantz, H. D. Newman, and F. H. Stigale, *J. Appl. Polym. Sci.*, **16,** 1249 (1972).
6. V. Tan and M. R. Kamal, *J. Appl. Polym. Sci.*, **22,** 2341 (1978).
7. M. Burke, R. J. Young, and J. L. Stanford, *Plast. Rubb. Proc. Appl.*, **20,** 121 (1993).
8. A. Conix, *Makromol. Chem.*, **26,** 226 (1958).
9. G. Menges, *Int. Polym. Sci. and Tech.*, **20,** T/20 (1993).
10. S. Berkowitz, *J. Appl. Polym. Sci.*, **29,** 4353 (1984).
11. C. V. Uglea and A. Mihaescu, *J. Chem. Tech. Biotechnol.*, **35A,** 1 (1985).
12. L. H. Buxbaum, *Angew Chem. Int. Ed.*, **7,** 182 (1968).
13. H. Zimmermann, in *Developments in Polymer Degradation,* Vol. 5, N. Grassie, Ed., Applied Science Publishers, London, 1977, p. 79.
14. I. Luderwald, H. Urrutia, H. Herlinger, and P. Hirt, *Angew. Makromol. Chem.*, **50,** 163 (1976).
15. I. Goodman and B. F. Nesbitt, *Polymer,* **1,** 384 (1960).
16. L. H. Peebles, M. W. Huffman, and C. T. Ablett, *J. Polym. Sci., A-1,* **7,** 479 (1969).
17. W. S. Ha and Y. K. Choun, *J. Polym. Sci., Polym. Chem. Ed.*, **17,** 2103 (1979).

Received June 29, 1995
Accepted January 5, 1996